THE JOURNAL OF BIOLOGICAL CHEMISTRY VOL. 284, NO. 24, pp. 16679–16692, June 12, 2009

Zebrafish *eaf1* and *eaf2/u19* Mediate Effective Convergence and Extension Movements through the Maintenance of *wnt11* and *wnt5* Expression

Received for publication, December 26, 2008, and in revised form, April 16, 2009 Published, JBC Papers in Press, April 20, 2009, DOI 10.1074/jbc.M109.009654

Jing-Xia Liu[‡1], **Bo Hu**[‡], **Yang Wang**[§], **Jian-Fang Gui**[§], **and Wuhan Xiao**[‡2]

From the [‡]*Key Laboratory of Biodiversity and Conservation of Aquatic Organisms and the* [§]*State Key Laboratory of Fresh Water Ecology and Biotechnology, Institute of Hydrobiology, Chinese Academy of Sciences, Wuhan 430072, China*

Studies have attributed several functions to the Eaf family, including tumor suppression and eye development. Given the potential association between cancer and development, we set forth to explore Eaf1 and Eaf2/U19 activity in vertebrate embryogenesis, using zebrafish. *In situ* hybridization revealed similar *eaf1* and *eaf2/u19* expression patterns. Morpholino-mediated knockdown of either *eaf1* or *eaf2/u19* expression produced similar morphological changes that could be reversed by ectopic expression of target or reciprocal-target mRNA. However, combination of Eaf1 and Eaf2/U19 (Eafs)-morpholinos increased the severity of defects, suggesting that Eaf1 and Eaf2/U19 only share some functional redundancy. The Eafs knockdown phenotype resembled that of embryos with defects in convergence and extension movements. Indeed, knockdown caused expression pattern changes for convergence and extension movement markers, whereas cell tracing experiments using *kaeda* mRNA showed a correlation between Eafs knockdown and cell migration defects. Cardiac and pancreatic differentiation markers revealed that Eafs knockdown also disrupted midline convergence of heart and pancreatic organ precursors. Noncanonical Wnt signaling plays a key role in both convergence and extension movements and midline convergence of organ precursors. We found that Eaf1 and Eaf2/U19 maintained expression levels of *wnt11* and *wnt5*. Moreover, *wnt11* or *wnt5* mRNA partially rescued the convergence and extension movement defects occurring in *eafs* morphants. Wnt11 and Wnt5 converge on *rhoA*, so not surprisingly, *rhoA* mRNA more effectively rescued defects than either *wnt11* or *wnt5* mRNA alone. However, the ectopic expression of *wnt11* and *wnt5* did not affect *eaf1* and *eaf2/u19* expression. These data indicate that *eaf1* and *eaf2/u19* act upstream of noncanonical Wnt signaling to mediate convergence and extension movements.

EAF1 (ELL-associated factor 1) was first discovered through its ability to associate with the protein ELL (eleven-nineteen lysine-rich leukemia), a fusion partner of MLL in the t(11; 19)(q23;p13.1) chromosomal translocation associated with acute myeloid leukemia (1, 2). Subsequent studies found a second binding partner for ELL, EAF2, which was independently identified as an androgen up-regulated gene in the rat prostate and named human up-regulated 19 (U19) (3, 4). ELL binds to RNA polymerase II and acts as a transcriptional elongation factor whose targeted deletion leads to embryonic lethality in mice (5, 6). Both EAF1 and EAF2, which share significant sequence homology, stimulate ELL elongation activity (7). Studies by Luo *et al.* (8) argued that EAF proteins are important in MLL-ELL leukemogenesis, whereas our previous studies showed that EAF2/U19 inhibits xenograft prostate tumor growth and undergoes down-regulation in prostate cancer cell lines (9). These findings link the *EAF2/U19* gene with two major human cancers: prostate cancer and acute myeloid leukemia. To investigate the function *EAF2/U19 in vivo*, we constructed a murine knock-out model. The *EAF2/U19* knock-out mice develop B-cell lymphoma, lung adenocarcinoma, hepatocellular carcinoma, and prostate intraepithelial neoplasia with high frequency (10). In addition, we demonstrated that EAF2/U19 could bind to and stabilize the classic tumor suppressor-pVHL (11). These findings further support *EAF2/U19* as a potential tumor suppressor; however, the molecular mechanisms underlying this activity remain poorly defined.

Evidence suggests that oncogenes and tumor suppressors may play a role in normal vertebrate embryogenesis. Thus, the evaluation of how these proteins function during embryogenesis would not only lead to a better understanding of development but may also shed light on how these proteins contribute to tumor initiation and progression (12, 13). Several studies have shown that *eaf2/u19* appears to be important during embryogenesis, particularly in eye development (14, 15), but its function in vertebrate embryogenesis remains unclear.

In vertebrates, the body plan is established during gastrulation by a set of morphogenetic processes, including epiboly, internalization, and convergence and extension movements (16). Gastrulation starts with the epiboly of the enveloping layer and deep cells and the internalization of prospective mesendodermal cells, followed by convergence and extension movements. convergence and extension movements narrow embryonic tissues mediolaterally and lengthen them anteroposteriorly (17). By convergence movements, the precursor cells of many organs migrate toward midline from bilateral tissues and assemble to form the primitive organs (18, 19). During the convergence and extension movements, multiple signaling cascades control coordinated cell behaviors. *silberblick/wnt11* (*slb*) and *pipetail/wnt5* (*ppt*) zebrafish mutants show abnormal

[1] Supported by National Natural Science Foundation of China (NSFC) (Youth Foundation) Grant 30700440 and Grant 20890113.
[2] Supported by "973" Grants 2004CB117404, 2007CB815705, and 2006CB504100; NSFC Grant 30671037; and Chinese Academy of Sciences Grant KSCX2-YW-N-020. To whom correspondence should be addressed. Fax: 86-27-68780087; E-mail: w-xiao@ihb.ac.cn.

convergence and extension movements and display a short tail and body axis (20, 21). Thus, the noncanonical Wnt cascade has been proposed to be essential for convergence and extension movements. In addition, *rhoA* has been reported to act downstream of *wnt5* and *wnt11* to regulate convergence and extension movements (22).

We employed the zebrafish embryo as a model system to investigate the role of *eaf1* and *eaf2/u19* in vertebrate development. Based on initial findings, we focused our examination on the regulation of convergence and extension movements and midline convergence of the heart and pancreas primordia by Eaf1 and Eaf2/U19 during zebrafish embryogenesis. We also examined whether *eaf1* and *eaf2/u19* regulate convergence and extension movements by noncanonical Wnt signaling.

EXPERIMENTAL PROCEDURES

Maintenance of Fish Stocks and Embryo Collection—Breeding wild-type zebrafish (*Danio rerio*) (AB) were maintained and embryos rose under standard library conditions (23). Embryos were collected and staged as described (24).

Cloning of Zebrafish eaf1 and eaf2—Zebrafish *eaf1* and *eaf2/u19* genes (GenBank™ accession numbers AAI53593 and CAQ15588, respectively) were identified using human orthologue sequences to search the zebrafish Ensembl data base (available on the World Wide Web). To amplify zebrafish *eaf1* and *eaf2/u19*, we used primers based on their cDNA open reading frame sequences. The primers for *eaf1* were 5′-GGTACCGATGAACGGCAGCTCGAACC-3′ and 5′-CCCGGGCGTCGATGTCGCTGTCACTGC-3′. The primers for *eaf2/u19* were 5′-GGTACCGTGGATTAGAATGAATGGAACAGC-3′ and 5′-CCCGGGCGTCATCATCGCTTTCACTTCCA-3′. Total RNA was isolated from zebrafish embryos using the RNeasy minikit (Qiagen), and cDNA was synthesized by the RevertAid™ first strand cDNA synthesis kit (Fermentas). The complete coding sequences were PCR-amplified, subcloned into the pTA2 vector (Toyobo), and then sequenced.

Whole Mount in Situ Hybridization—Probes for identifying zebrafish, *eaf1*, *eaf2/u19*, *ntl*, *hgg*, *lefty2*, *gata5*, *foxo5*, *gsc*, *chd*, *foxa3*, *bon*, and *sox17* by *in situ* hybridization were PCR-amplified from cDNA pools using the appropriate sets of primers (sequences provided upon requested). Probes for *otx1*and *dlx3b* were generous gifts from Dr. T. Whitefield (Medical Research Council Centre for Developmental and Biomedical Genetics, Sheffield, UK) (25). Dr Z. Yin (Institute of Hydrobiology, Chinese Academy of Sciences, Wuhan, China) kindly provided probes for *myoD*, *papc*, *bmp4*, *amhc*, *vmhc*, *cmlc*, *insulin*, *pdx-1*, *wnt5*, and *wnt11*. The procedure for whole mount *in situ* hybridization was performed as described previously (26).

Morpholinos and mRNA Injection and Rescue Experiments—Two nonoverlapping, translation-blocking morpholinos (MOs)[3] targeting the zebrafish *eaf1* gene (Eaf1-MO1, GCGGCGGGTTCGAGCTGCCGTTCAT; Eaf1-MO2, GAATTCACCAACTTCACCCAAAATG; two nonoverlapping, translation-blocking morpholinos targeting the zebrafish *eaf2* gene (Eaf2-MO1, ATATGCTGTTCCATTCATTCTAATC; Eaf2-MO2, TAGCGATTTTCAACTTTCTGCTTGG), and a standard control (STD) morpholino (CCTCTTACCTCAGTTACAATTTATA) were purchased from Gene Tools, LLC (Philomath, OR). All morpholinos were resuspended in 1× Danieau medium (58 mM NaCl, 0.7 mM KCl, 0.4 mM $MgSO_4$, 0.6 mM $Ca(NO3)_2$, and 5.0 mM HEPES, pH 7.6) and injected into embryos at the one-cell stage.

The full-length zebrafish *eaf1* cDNA was cloned into pEGFP-N1 (Clontech) to generate wild-type Eaf1 tagged with GFP at the carboxyl terminus (WT) to validate the efficiency of Eaf1-MO1. The zebrafish GFP-tagged mutated Eaf1 (MT) was generated by PCR using a forward primer with five mismatched nucleotides, 5′-GGTACCGATGAGCCGCTGGTGGAACCCGCCGCTGG-3′ (mismatched nucleotides are underlined) to test for specificity of Eaf1-MO1. The full-length zebrafish *eaf2/u19* cDNA was also cloned into pEGFP-N1 (Clontech) to generate GFP-tagged wild-type Eaf2/U19 (WT) to validate efficiency of Eaf2-MO1. The zebrafish GFP-tagged mutated Eaf2/U19 (MT) was generated by PCR using a forward primer with five mismatched nucleotides, 5′-GGTACCGTCGAATCGAATGATTCGAACAGCATATTCAAAC-3′ (mismatched nucleotides are underlined) to test the specificity of Eaf2-MO1.

For ectopic expression of zebrafish *eaf1* (*zEaf1*), *eaf2/u19* (*zEaf2*), *wnt11*, and *wnt5* in embryos, full-length wild-type *eaf1*, *eaf2/u19, wnt11*, and *wnt5* were subcloned into the Psp64 poly(A) vector (Promega). Capped mRNAs were synthesized using the Ampticap SP6 High Yield message maker kit (Epicenter). Capped mRNA (200–500 pg) was injected into one-cell stage embryos.

For the rescue experiments, full-length wild-type cDNAs of zebrafish *eaf1* (*zEaf1*), zebrafish *eaf2/u19* (*zEaf2*), human *EAF1* (*hEaf1*), human *EAF2/U19* (*hEaf2*), zebrafish *wnt5*, zebrafish *wnt11*, and zebrafish wild-type *rhoA* (provided by Zhan Yin) were subcloned into the Psp64 poly(A) vector (Promega). To avoid quenching by the Eaf1-MO1 in these rescue experiments, we used a primer to introduce five mismatched nucleotides in the zebrafish *eaf1* mRNA, 5′-AAGCTTATGAATGGATCTTCGAACCCGCCGCTG-3′ (mismatched nucleotides are underlined), but Eaf2-MO1 itself has seven nucleotides mismatching to zebrafish *eaf2/u19* open reading frame, so it cannot quench the zebrafish *eaf2/u19* mRNA. Capped mRNAs synthesized using the Ampticap SP6 High Yield message maker kit (Epicenter) mixed with corresponding morpholinos were co-injected into one-cell stage embryos. Different amounts of synthetic mRNA, varying from 10 to 200 pg, were titrated by co-injection with morpholinos to reach an optimal level that could rescue the defects of the *eaf1* and *eaf2/u19* morphants effectively. All of the microinjection was performed using a Harvard apparatus PLI-100.

Semiquantitative RT-PCR—Using the RNeasy minikit (Qiagen), we isolated total RNAs from embryos at the 50% epiboly stage that had been injected with *eaf1* mRNA, *eaf2* mRNA, GFP mRNA, Eafs-MO1(Eaf1-MO1 + Eaf2-MO1), or a standard morpholino (STD-MO). Aliquots of RNA were subjected to 1% agarose gel electrophoresis and stained by ethidium bromide to verify RNA quantity and quality. For RT-PCR detection, about

[3] The abbreviations used are: MO, morpholino; WT, wild type; GFP, green fluorescent protein; RT, reverse transcription; hpf, hours postfertilization; STD-MO, standard morpholino.

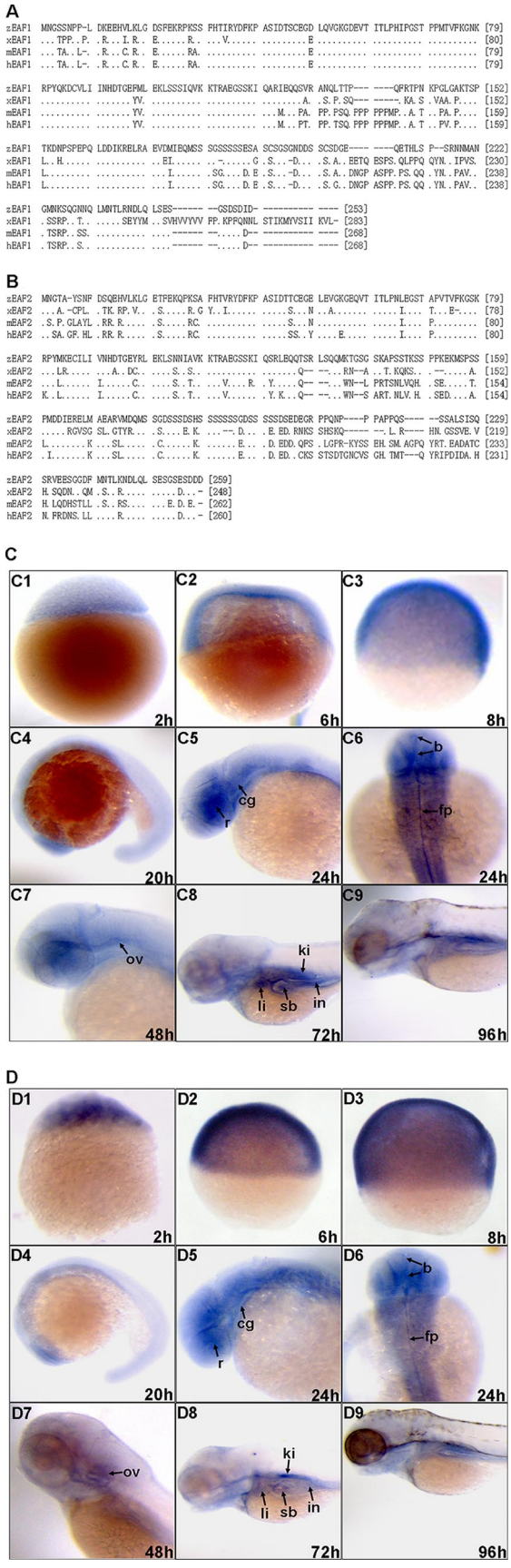

FIGURE 1. **Alignment and expression of zebrafish (*D. rerio*) Eaf1 and Eaf2/U19.** *A*, zebrafish *eaf1* (*zEAF1*; GenBank™ accession number AAI53593) codes for a 253-amino acid protein with orthologues in *X. laevis* (*xEAF1*; GenBank™ accession number AAI25802), *Mus musculas* (*mEAF1*; GenBank™ accession number AAH41329), and *Homo sapiens* (*hEAF1*; GenBank™ accession number AAH79658). *B*, zebrafish *eaf2/u19* (*zEAF2*; GenBank™ accession number CAQ15588) codes for a 259-amino acid protein with orthologues in *X. laevis* (*xEAF2*; GenBank™ accession number CAE22450), *M. musculas* (*mEAF2*; GenBank™ accession number AAH04721), and *H. sapiens* (*hEAF2*; GenBank™ accession number AAO63811). *C*, whole mount *in situ* hybridization analysis of zebrafish *eaf1* expression. *D*, whole mount *in situ* hybridization analysis of zebrafish *eaf2/u19* expression. *C1* and *D1*, blastula stage, lateral view; *C2* and *D2*, shield stage embryos, lateral view; *C3* and *D3*, 75% epiboly, lateral view; *C4* and *D4*, 20 hpf, lateral view with anterior to the *left*; *C5* and *D5*, 24 hpf, lateral view with anterior to the *left*; *C6* and *D6*, 24 hpf, dorsal view with anterior on *top*; *C7* and *D7*, 48 hpf, lateral view with anterior to the *left*; *C8* and *D8*, 72 hpf, lateral view with anterior to the *left*; *C9* and *D9*, 96 hpf, lateral view with anterior on *top*. *b*, brain; *cg*, cranial ganglion; *fp*, floor plate; *ki*, kidney; *in*, intestine; *li*, liver; *sb*, swim bladder; *r*, retina; *ov*, otic vesicle.

1 μg of each RNA was reverse transcribed by the reverse transcriptase Moloney murine leukemia virus (Invitrogen) at 37 °C with oligo(dT) primers. We used 18 S RNA to adjust the concentrations of these first strand cDNAs so they could be used as templates for semiquantitative PCR. PCR reactions using gene-specific primers were carried out in a Chromo 4™ detector for the PTC DNA Engine™ system (Bio-Rad) in the presence of SYBR green. All PCRs were run in triplicate and repeated at least three times. Differences were calculated according to the $\Delta\Delta Ct$ relative quantization method using 18 S RNA as calibrators. The primers for the zebrafish *wnt5* (*wnt5b*) gene were 5′-CTTCGCCCGGGAGTTTGTGGA-3′ and 5′-CGGCGGCGCTGTCGTATTTC-3′. The primers for zebrafish *wnt11* gene were 5′-CCGTCTTCACCAATAGACCTTG-3′ and 5′-CCCAGTCTCTTCCCCTCAGT-3′. The primers for zebrafish 18 S were 5′-GAGAAACGGCTACCACATCC-3′ and 5′-CACCAGACTTGCCCTCCAA-3′.

Cell Tracing Experiments—For the cell tracing experiments, full-length wild-type *kaeda* was subcloned into the pCS2+ vector (27). Capped mRNA was synthesized using the Ampticap SP6 High Yield message maker kit (Epicenter). 200 pg of capped *kaeda* mRNA was co-injected with STD-MO or Eafs-MO1 (Eaf1-MO1 + Eaf2-MO1, 4 ng + 4 ng) into one-cell stage embryos. Injected embryos were maintained in a dark room until the shield stage. To convert green fluorescence to red, a beam of UV light, generated by a UV filter set (350 – 400 nm) on a Zeiss fluorescence microscope was directed for 1 s at the dorsal or lateral blastoderm margin of embryos (27). The location of red fluorescent cells was then photographed at the indicated time points using the Zeiss fluorescence microscope.

RESULTS

Expression of eaf1 and eaf2/u19 during Zebrafish Development—We chose the zebrafish model to examine the function of *eaf1* and *eaf2/u19* during vertebrate development. An orthologous gene search of the zebrafish Ensembl data base with human *EAF1* and *EAF2/U19* sequences yielded a single copy of each gene. We then cloned the zebrafish *eaf1* and *eaf2/u19* genes by RT-PCR. Zebrafish *eaf1* encodes a predicted protein 253 amino acids in length that has a high degree of identity with *Eaf1* from *Xenopus* (67.83%), mice (74.44%), and humans (74.81%), with the amino terminus (amino acids 21–126) exhibiting much greater conservation than the carboxyl terminus (Fig. 1*A*). Similarly, the predicted protein encoded by zebrafish

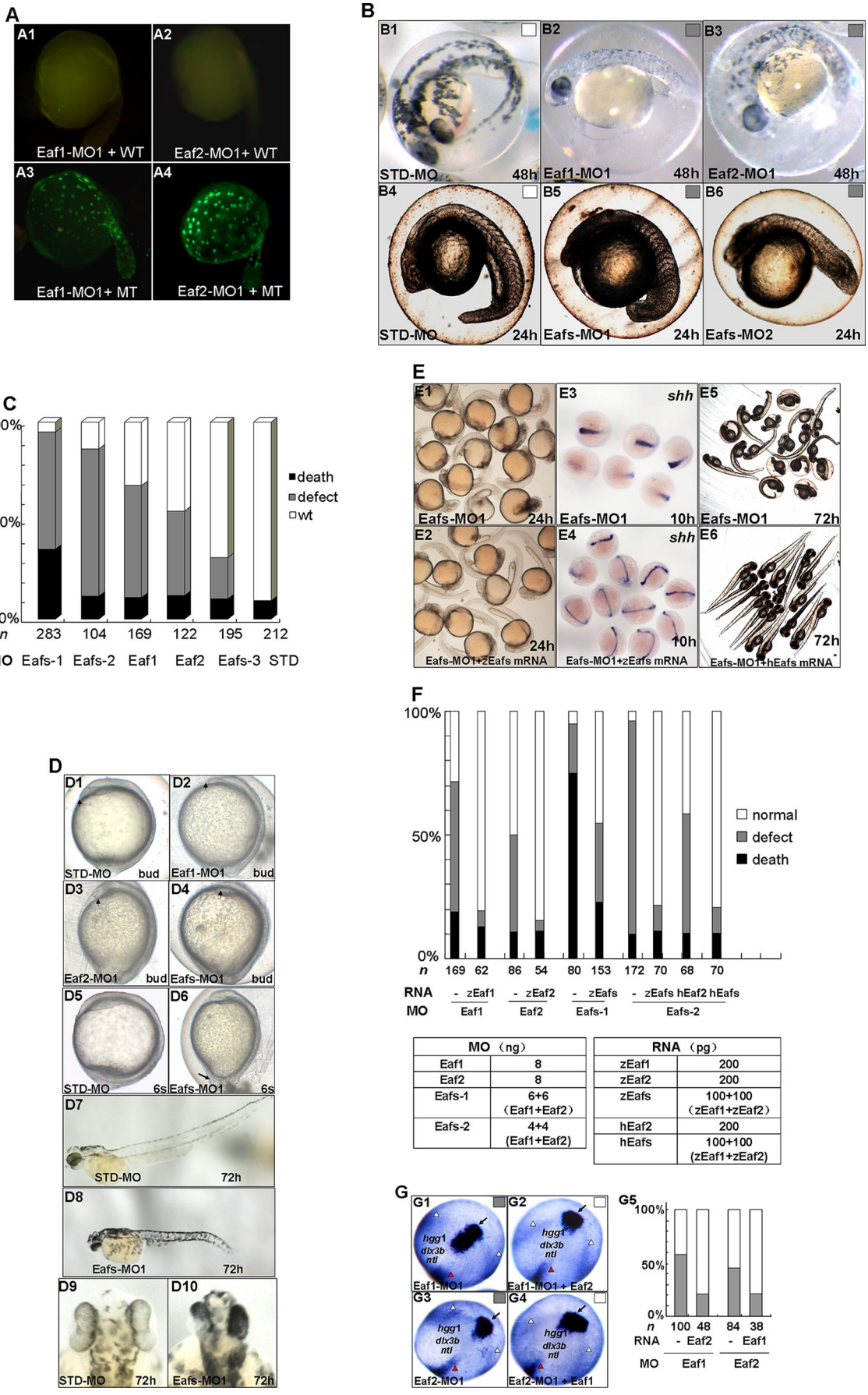

MO (ng)	
Eaf1	8
Eaf2	8
Eafs-1	6+6 (Eaf1+Eaf2)
Eafs-2	4+4 (Eaf1+Eaf2)

RNA (pg)	
zEaf1	200
zEaf2	200
zEafs	100+100 (zEaf1+zEaf2)
hEaf2	200
hEafs	100+100 (zEaf1+zEaf2)

eaf2/u19 is 259 amino acids in length and has a high degree of identity with *Eaf2/U19* from *Xenopus* (62.31%), mice (62.08%), and humans (64.04%). Again we found that the greatest degree of conservation occurred in the amino terminus (amino acids 29–126) (Fig. 1*B*).

Examination of zebrafish embryos by *in situ* hybridization revealed a similar pattern of expression for embryonic *eaf1* and *eaf2/u19* as well as for maternal transcripts in all cells at early developmental stages (Fig. 1, C (*C1*, *C2*, and *C3*) and D (*D1*, *D2*, and *D3*)). By 20 h postfertilization (hpf), the anterior head region expressed the highest level of *eaf1* and *eaf2/u19*, whereas other regions of the body expressed lower, homogenous levels (Fig. 1, *C* (*C4*) and *D* (*D4*)). By 24 hpf, *eaf1* and *eaf2/u19* transcripts were predominantly distributed in the central and ventral nervous system, including the brain, cranial ganglion, retina, otic vesicle, and floor plate (Fig. 1, *C* (*C5* and *C6*) and *D* (*D5* and *D6*)). By 48 hpf, the strongest signals were still distributed in the central nervous system and sensory organs (Fig. 1, *C* (*C7*) and *D* (*D7*)). The expression of *eaf1* and *eaf2/u19* in the nervous system became weaker by 72 hpf and remained low at 96 hpf. At the same time, expression increased in strength at sites with an active interaction between the epithelium and mesenchyme, such as the liver, kidney, swim bladder, and intestine (Fig. 1, *C* (*C8* and *C9*) and *D* (*D8* and *D9*)).

Morpholino-mediated Knockdown of eaf1 and eaf2/u19 Results in Abnormal Axis Formation and Disrupted Convergence and Extension Movements during Gastrulation—To investigate the roles of *eaf1* and *eaf2/u19* during zebrafish embryogenesis, we knocked down their expression using translation-blocking morpholinos. As a first step, we evaluated the efficiency of the morpholino targeting *eaf1* (Eaf1-MO1) and *eaf2/u19* (Eaf2-MO1) by co-injecting each into zebrafish embryos along with a vector expressing the target protein tagged with GFP at the carboxyl terminus. We also evaluated the specificity by co-injecting the morpholinos with vectors expressing a mutated form of GFP-tagged Eaf1 or Eaf2/U19; each *eaf* target sequence had five mismatched nucleotides in the 5′ region. Eaf1-MO1 (8 ng) and Eaf2-MO1 (8 ng) successfully blocked expression of GFP-tagged Eaf1 and Eaf2/U19, respectively, but not expression of the mutated targets (Fig. 2*A*).

We next injected Eaf1-MO1 (8 ng) or Eaf2-MO1 (8 ng) into zebrafish embryos at the one-cell stage and evaluated morphology at 48 hpf. Knockdown of Eaf1 and Eaf2 resulted in a similar phenotype; both morphants had a shorter tail and a reduced head as compared with the control embryo injected with STD-MO (Fig. 2*B* (*B1–B3*)). A combination of 4 ng each of Eaf1-MO1 and Eaf2-MO1 (Eafs-MO1) produced a more severe defect in the *eafs* morphants (Fig. 2*B* (*B4* and *B5*)). To validate the effects seen with Eaf1-MO1 and Eaf2-MO1, we repeated the assay using two additional nonoverlapping, translation-blocking morpholinos targeting *eaf1* and *eaf2/u19* mRNA: Eaf1-MO2 and Eaf2-MO2. Injections with the individual morpholinos (data not shown) or a combination of both resulted in a phenotype similar to what was seen with Eaf1-MO1 and Eaf2-MO1 (Fig. 2*B* (*B6*)). Next, embryos were injected with varying amounts of Eaf1-MO1 and/or Eaf2-MO1 to determine if the changes in morphology occurred in a dose-dependent manner. We evaluated the embryos at 24 hpf for viability and at 3 days postfertilization for defects; Fig. 2*C* clearly shows a dose-dependent effect.

We further characterized the morphological changes seen with Eaf1 and Eaf2/U19 knockdown. Embryos at the one-cell stage were injected with a total of 8 ng of morpholinos (Eaf1-MO1, Eaf2-MO1, or a combination of both) and then examined at different stages: at the bud stage (Fig. 2*D* (*D1–D4*)), at the six-somite stage (Fig. 2*D* (*D5* and *D6*)), and at 72 hpf (Fig. 2*D* (*D7–D10*). Knockdown of expression of the *eaf1* and *eaf2/u19* genes resulted in a shorter anterior-posterior axis of body (Fig. 2*D* (*D1–D6*)), which resembled the convergence and extension defects seen with knockdown of *wnt11* gene expression (28). Moreover, embryos injected with Eafs-MO1 had a shorter tail and a fusion of the eyes, resembling that of *slb/wnt11* mutants (20).

FIGURE 2. **Knockdown of Eaf1 and Eaf2/U19 caused defects in gastrulation.** *A*, validation of the morpholinos. *A1*, embryos were injected with Eaf1-MO1 (8 ng) and a wild-type *eaf1*-GFP fusion protein expression vector (*WT*) and then examined by fluorescence microscopy. *A2*, embryos were injected with Eaf2-MO1 (8 ng) and a wild-type *eaf2/u19*-GFP fusion protein expression vector. *A3*, embryos were injected with Eaf1-MO1 and a mutated *eaf1*-GFP fusion protein expression vector (*MT*). *A4*, embryos were injected with Eaf2-MO1 and a mutated *eaf2/u19*-GFP fusion protein expression vector. *B*, morphology of representative morphants. *B1* and *B4*, morphants of the STD-MO (8 ng) at 48 hpf (*B1*) and 24 hpf (*B4*). *B2*, an *eaf1* morphant (Eaf1-MO1; 8 ng) at 48 hpf. *B3*, an *eaf2/u19* morphant (Eaf2-MO1; 8 ng) at 48 hpf. *B5*, an *eafs* morphant (Eaf1-MO1 plus Eaf2-MO1; 4 ng each) at 24 hpf. *B6*, an *eafs* morphant 2 (Eaf1-MO2 plus Eaf2-MO2; 4 ng each) at 24 hpf. *C*, embryos were injected with morpholinos: Eafs-1 (Eaf1-MO1 plus Eaf2-MO1; 6 ng each), Eafs-2 (Eaf1-MO1 plus Eaf2-MO1; 4 ng each), Eaf1 (Eaf1-MO1, 8 ng), Eaf2 (Eaf2-MO1, 8 ng), Eafs-3 (Eaf1-MO1 and Eaf2-MO1, 2 ng each), and STD-MO (8 ng). *Black box*, dead embryos at 24 hpf; *gray box*, embryos with defects at 3 days postfertilization (*dpf*) with defects characterized by mild cyclopia, no forebrain structures anterior to the eyes, and reduced body length; *white box*, embryos with no discernable defects. *D*, morpholinos, including Eaf1-MO1 (8 ng), Eaf2-MO1 (8 ng), Eafs-MO1 (Eaf1-MO1 plus Eaf2-MO1; 4 ng each), and STD-MO (8 ng) were injected at the one-cell stage, and the morphology was assessed at different embryonic stages. *D1*, *D2*, *D3*, and *D4*, bud stage embryos, lateral view, dorsal to the *right*; the *arrowhead* marks the anterior-most structure. *D5* and *D6*, six somite stage embryos, lateral view, dorsal to the *right*. The *arrow* indicates the misprotruded tail. *D7* and *D8*, 72 hpf, lateral view, anterior to the *left*. *D9* and *D10*, 72 hpf, dorsal view, anterior to the *top*. *E*, both zebrafish and human *eaf1* and *eaf2/u19* mRNA completely rescued the Eaf1-MO1-, Eaf2-MO1-, and Eafs-MO1 (Eaf1-MO1 plus Eaf2-MO1)-induced defects. *E1* and *E2*, 24 hpf, morphology of embryos injected with Eafs-MO1 alone and injected with Eafs-MO1 combined with both zebrafish *eaf1* and *eaf2/u19* mRNA (*zEafs mRNA*). *E3* and *E4*, 10 hpf, whole mount *in situ* hybridization assays for *shh* expression in embryos treated as the same as that of *E1* and *E2*. *E5* and *E6*, 72 hpf, morphology of embryos injected with Eafs-MO1 alone and injected with Eafs-MO1 combined with human *Eaf1* and *Eaf2/U19* mRNA (*hEafs mRNA*). *F*, the embryos were scored morphologically from four independent experiments. *Black bar*, percentage of death; *gray bar*, percentage of defects; *white bar*, percentage of embryos with no discernable defects. The dosage and composition of the injected mRNA and morpholino are indicated. To eliminate error among different experiments, we used the same batch of embryos produced by a select number of zebrafish. *G*, *eaf1* mRNA rescued Eaf2-MO-mediated convergence and extension movement defects during gastrulation, and *eaf2/u19* mRNA rescued Eaf1-MO-mediated convergence and extension movement defects during gastrulation. *G1*, Eaf1-MO1 (8 ng)-injected embryos stained with the markers *ntl*, *hgg*, and *dlx3b*. *G2*, Eaf1-MO1 (8 ng) plus *eaf2/u19* mRNA (50–100 pg)-injected embryos stained with the markers *ntl*, *hgg*, and *dlx3b*. *G3*, Eaf2-MO1 (8 ng)-injected embryos stained with the markers *ntl*, *hgg*, and *dlx3b*. *G4*, Eaf2-MO1 (8 ng) plus *eaf1* mRNA (50–100 pg)-injected embryos stained with the markers *ntl*, *hgg*, and *dlx3b*. *Black arrow*, prechordal plate (stained by *hgg* probe); *white arrowhead*, edges of the neural plate (stained by *dlx3b*); *red arrowhead*, axial chorda (stained by *ntl*). All embryos are shown at 9 hpf in dorsal view, anterior to the *top*. *G5*, the ratio of defects in convergence and extension movements rescued by *eaf1* and *eaf2/u19* mRNA was scored by the three markers, *hgg1*, *dlx3b*, and *ntl*.

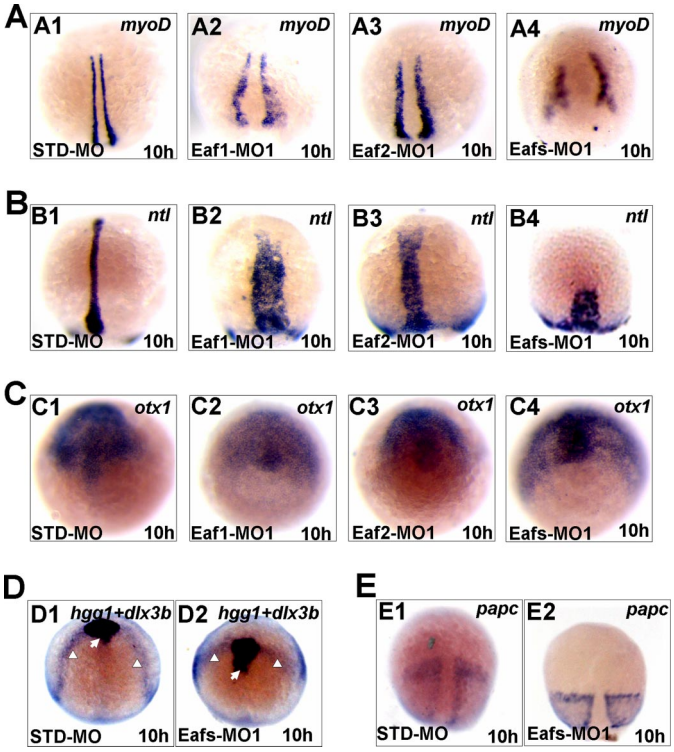

FIGURE 3. **Whole mount *in situ* hybridization assays for different markers in 10-hpf-old embryos injected with STD-MO, Eaf1-MO1, Eaf2-MO1, or Eafs-MO1 (Eaf1-MO1 plus Eaf2-MO1).** *A*, *myoD* (staining the adaxial cell). *B*, *ntl* (staining the forerunner cell group, axial chorda mesoderm). *C*, *otx1* (staining the anterior axial hypoblast and neural plate). *D*, *dlx3b* (*white arrowheads*) and *hgg* probe (staining the prechordal plate, indicated by *white arrows*). *E*, *papc* (staining the paraxial mesoderm). Shown are dorsal views with the anterior to the *top*.

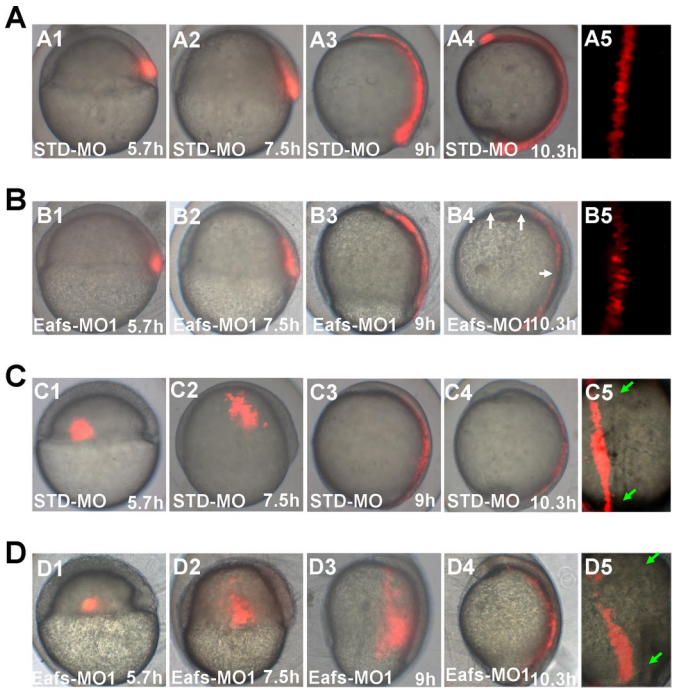

FIGURE 4. **Eaf1 and Eaf2/U19 were required for normal convergence and extension movements during gastrulation.** *A* and *B*, knockdown of Eafs (Eaf1 and Eaf2/U19) disrupted extension of mesendoderm. *C* and *D*, knockdown of Eafs disrupted convergence. *kaede* mRNA (200 pg) was co-injected with 8 ng of the indicated MOs into wild-type embryos. Cell labeling was performed by UV activation of *kaede* at 5.7 hpf. Pictures were taken directly after labeling. *A* and *C*, STD-MO; *B* and *D*, eafs-MO1; *A1*, *B1*, *C1*, and *D1*, shield (6 hpf); *A2*, *B2*, *C2*, and *D2*, 60% epiboly (7.5 hpf); *A3*, *B3*, *C3*, and *D3*, 90% epiboly (9 hpf); *A4*, *B4*, *C4*, and *D4*, bud (10.3–10.5 hpf); *A5*, *B5*, *C5*, and *D5*, bud, dorsal view with the anterior to the *top*. Each experiment was repeated five times. *B4*, the gaps of labeling extension mesendoderm cells are indicated by *white arrows*. *A5* and *B5*, magnification of chordal region in *A4* and *B4*, respectively. *C5* and *D5*, dorsal view of the labeling convergence cells of *C4* and *D4*, respectively, chorda indicated by *green arrows*.

Rescue experiments represent the gold standard for demonstrating a direct relationship between morpholino-mediated knockdown of a specific protein and the changes in phenotype attributed to the knockdown. Thus, we injected embryos with Eafs-MO1 alone or with Eafs-MO1 mixed with capped zebrafish full-length *eaf1* mRNA and/or *eaf2/u19* mRNA. To avoid quenching, the *eaf1* mRNA contained five mismatched synonym nucleotides, whereas the *eaf2/u19* mRNA could not be quenched by Eaf2-MO1 due to seven nucleotides mismatched. Individually, both mRNAs rescued the phenotype induced by their "matched" MO (data not shown). Also, a mixture of *eaf1* and *eaf2/u19* mRNA (*zeafs*) rescued the phenotype of *eafs* morphants (Fig. 2, *E* (*E1* and *E2*) and *F*). We also evaluated *shh* expression as a marker for convergence and extension movements by *in situ* hybridization and showed that zebrafish *eaf1* and *eaf2/u19* mRNA also rescued convergence and extension movement defects (Fig. 2*E* (*E3* and *E4*)). Interestingly, human *EAF1* and *EAF2/U19* mRNA could also rescue the defects of *eafs* morphants, suggesting that its function is conserved across species (Fig. 2, *E* (*E5* and *E6*) and *F*).

The 57.25% amino acid identity between zebrafish Eaf1 and Eaf2/U19, their equivalent mRNA expression patterns during embryogenesis, and the similar phenotype produced by their knock-out supports the possibility of redundant functions for Eaf1 and Eaf2/U19 in development. To test this possibility, we did reciprocal rescue experiments in which embryos were co-injected with Eaf1-MO1 and varying amounts of *eaf2/u19* mRNA or with Eaf2-MO1 and varying amounts of *eaf1* mRNA. Embryos were then stained with markers for convergence and extension movement: *ntl* to show the axial chorda, *hgg* to show the prechordal plate, and *dlx3b* to show the edges of the neural plate. We found that 50–100 pg of *eaf2/u19* mRNA rescued Eaf1-MO1-mediated convergence and extension movement defects (Fig. 2*G* (*G1*, *G2*, and *G5*)). Similarly, 50–100 pg of *eaf1* mRNA rescued Eaf2-MO-mediated defects (Fig. 2*G* (*G3*–*G5*)). This suggested that Eaf1 and Eaf2/U19 performed some of the same functions in embryogenesis. However, the morpholinos did not induce higher expression of the reciprocal *eaf* mRNAs (data not shown), suggesting that the functions of the two were not completely redundant. This was not surprising, given that either Eaf1-MO1 or Eaf2-MO1 alone could induce a phenotype, which increased in severity upon combining the two morpholinos (Fig. 2, *B* and *C*).

Further Characterization of the Convergence and Extension Movement Defect Caused by eaf1 and eaf2/u19 Knockdown—To more thoroughly investigate convergence and extension movement defects, we used whole mount *in situ* hybridization to analyze the expression patterns of several marker genes. We found that knockdown of Eaf1, Eaf2/U19, or both caused a widening in the distance between bilateral adaxial cells, as visualized by mesodermal *myoD* expression, and the axial chorda

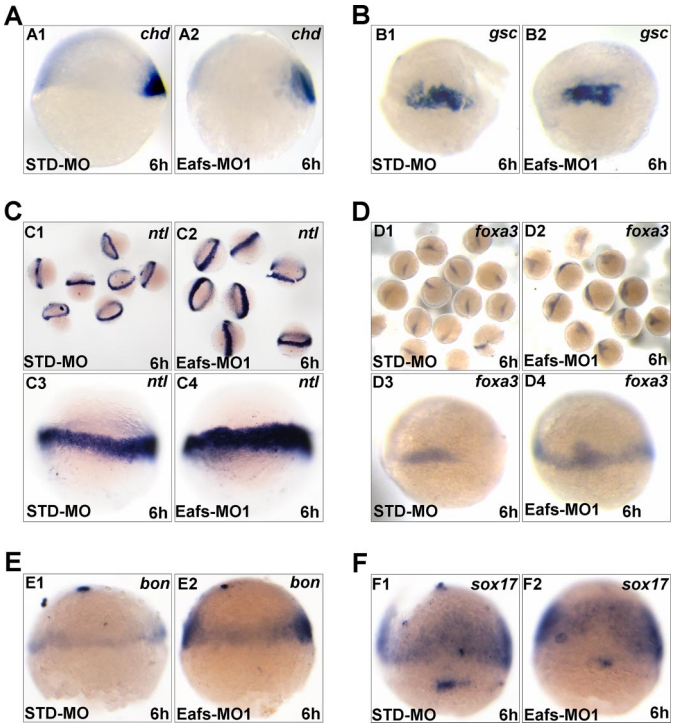

FIGURE 5. **Eaf1 and Eaf2/U19 knockdown did not affect cell fate specification at the beginning of gastrulation.** *A*, *chd* expression in embryos injected with STD-MO (*A1*) or Eafs-MO1 (*A2*). *B*, *gsc* expression in embryos injected with STD-MO (*B1*) or Eafs-MO1 (*B2*). *C*, *ntl* expression in embryos injected with STD-MO (*C1* and *C3*) or Eafs-MO1 (*C2* and *C4*). *D*, *foxa3* expression in embryos injected with STD-MO (*D1* and *D3*) or Eafs-MO1 (*D2* and *D4*). *E*, *bon* expression in embryos injected with STD-MO (*E1*) or Eafs-MO1 (*E2*). *F*, *sox17* expression in embryos injected with STD-MO (*F1*) or Eafs-MO1 (*F2*). Injected embryos were fixed at 6 hpf, and *in situ* hybridization was performed with the indicated probes, respectively. *A1*, *A2*, *C1–C4*, *E1*, and *E2*, lateral view, animal pole *top*; *B1*, *B2*, *D1–D4*, *F1*, and *F2*, dorsal-lateral view, animal pole *top*.

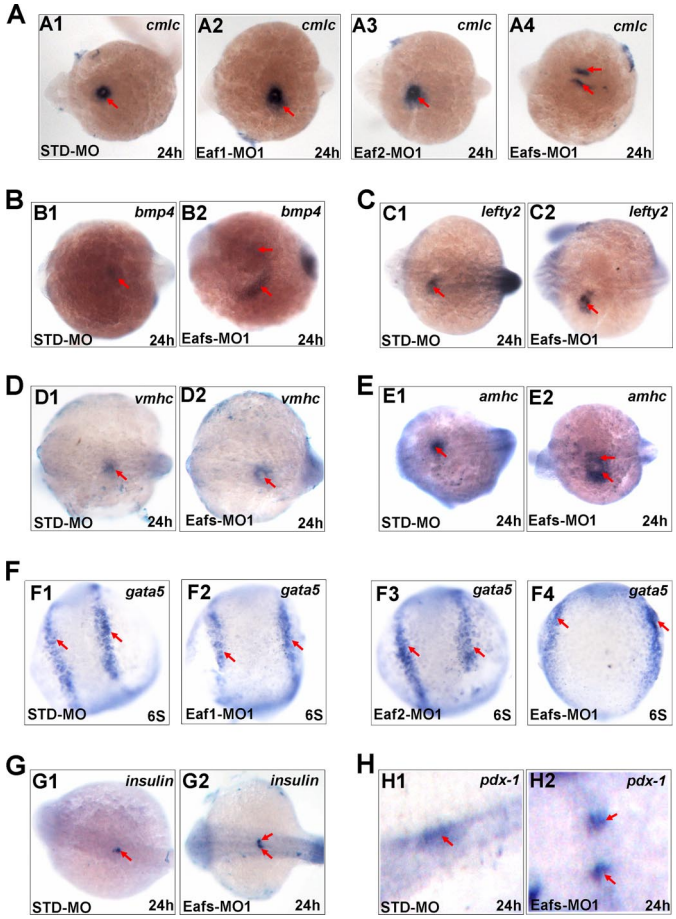

FIGURE 6. **Eaf1 and *eaf2/u19* regulated myocardial cell migration (*A–F*) and midline convergence of pancreas precursors (*G* and *H*) without affecting their cell fate.** Shown is *cmlc* (*A1–A4*) *bmp4* (*B1* and *B2*), *lefty2* (*C1* and *C2*), *vmhc* (*D1* and *D2*), *amhc* (*E1* and *E2*), *gata5* (*F1–F4*), *insulin* (*G1* and *G2*), and *pdx-1* (*H1* and *H2*) expression in 24 hpf embryos injected with STD-MO or Eafs-MO1, in dorsal view, with anterior to the *left*. The *red arrows* in *A–F* indicate myocardial cells, and the *red arrows* in *G* and *H* indicate pancreas precursors.

mesoderm could not extend to reach the anterior region, as visualized by expression of the mesodermal marker *ntl* (Fig. 3, *A* and *B*). In addition, the neural plate, expressing the neuroectodermal marker *otx1*, became broader (Fig. 3*C*). As before, simultaneous knockdown of Eaf1 and Eaf2/U19 protein levels produced a phenotype similar to the one that resulted from knockdown of a single Eaf, but the double knockdown caused more severe defects in convergence and extension movements (Figs. 2, *B* (*B4*) and *C* (*C4*), and 3*A* (*A4*)). Furthermore, double knockdown of Eaf1 and Eaf2/U19 disrupted convergence of the edges of the neural plate, as visualized by *dlx3b* expression (Fig. 3*D*) and resulted in a more posterior positioned prechordal plate (staining by *hgg*) (Fig. 3*D*). Embryos injected with Eafs-MO1 also showed shorter presomitic mesoderm domains than controls (staining by *papc*) (Fig. 3*E*). The more severe phenotype observed in the double knockdown embryos indicates that Eaf1 and Eaf2/U19 have at least some nonoverlapping functions.

Role for Eaf1 and Eaf2/U19 in Cell Migration—To assess the effect of *eaf1* and *eaf2/u19* loss on cell migration, we performed cell tracing experiments using Eafs-MO1 and capped *kaeda* mRNA. The *kaeda* gene encodes a protein with green fluorescence that changes to a red upon stimulation with a beam of UV light (350–400 nm) (27). At 5.7 hpf, we directed the UV light at the dorsal shield of injected embryos to analyze the extension of axial mesoderm cells at the indicated time points (Fig. 4, *A* and *B*). In STD-MO-injected embryos, the labeled cells extended along the AP axis and intercalated in nonlabeled cells to form an elongated and interrupted cell array (Fig. 4*A* (*A4* and *A5*); $n = 3$). In addition, the AP length measured by labeled cells dramatically increased by the end of the gastrula period (Fig. 4*A* (*A3*)), and continued to increase during the segmentation period (Fig. 4*A* (*A4*)). In Eafs-MO1-injected embryos, the initial size of the labeled cells was the same as that in the STD-MO1-injected embryos, but its AP axis length was obviously shorter at the end of gastrulation (Fig. 4, *A* (*A3*) and *B* (*B3*)). Furthermore, the subsequent elongation of the labeled cells in the array during early segmentation was almost completely inhibited in the *eafs* morphants (Fig. 4*B* (*B4*); $n = 5$). The dorsal labeled cells in *eafs* morphants also displayed defects in polarization and intercalation (Fig. 4*B* (*B5*)). To measure dorsal-ward movements of lateral cells (convergence), a cluster of cells, located in the lateral margin, 90° from the dorsal shield, was labeled by UV light, and the dorsal translocation of the cells was analyzed at the indicated time points (Fig. 4, *C* and *D*). In STD-MO-injected embryos, the labeled cells reached the dorsal site,

along with the mediolateral axis at the end of gastrula period (Fig. 4*C* (*C3*)) and then underwent mediolateral intercalation with the axial tissue (Fig. 4*C* (*C4* and *C5*); $n = 5$). In contrast, the labeled cells in the *eafs* morphants remained at the lateral site with a broader distribution at the end of the gastrula period (Fig. 4*D* (*D3*)). At the early segmentation stage, although the labeled cells reached the dorsal site (Fig. 4*D* (*D4*)), they could not undergo mediolateral intercalation due to the long distance from the dorsal axis; thus, they could not get into the axial tissue (Fig. 4*D* (*D5*); $n = 5$). The extension of the lateral tissue was not inhibited, but it was disorganized (Fig. 4*D* (*D2–D4*)). The impaired dorsal-ward movements of lateral cells not only resulted in a significant reduction of the AP length (Fig. 2*B*) but also resulted in a shorter dorsal mesendoderm during gastrulation (Fig. 3*A*). Taken together, the analysis of cell migration and morphology provided evidence that both convergence and extension movements in lateral and dorsal regions of the gastrula require Eaf1 and Eaf2/U19.

Eaf1 and Eaf2/U19 Knockdown Does Not Affect Cell Fate Specification at Early Gastrula—To determine whether knockdown of Eaf1 and Eaf2/U19 could also affect cell fate specification at the beginning of gastrulation, we examined the expression of *chd* and *gsc*, two cell fate specification markers at early gastrula. In *eafs* morphants, the expression level of *chd* (Fig. 5*A* (*A2*)) and *gsc* (Fig. 5*B* (*B2*)) was not significantly changed compared with STD-MO-injected controls (Fig. 5*A* (*A1*) and 5*B* (*B1*)), resembling the results observed in *shp2* (29) and *csk* (30) morphants. Both *shp2* and *csk* have been showed to regulate convergence and extension movement without affecting cell fate specification during gastrulation.

Subsequently, we examined the expression of the panmesodermal marker *ntl*. As showed in Fig. 5*C*, the expression domain of *ntl* was apparently expanded (Fig. 5*C* (*C2* and

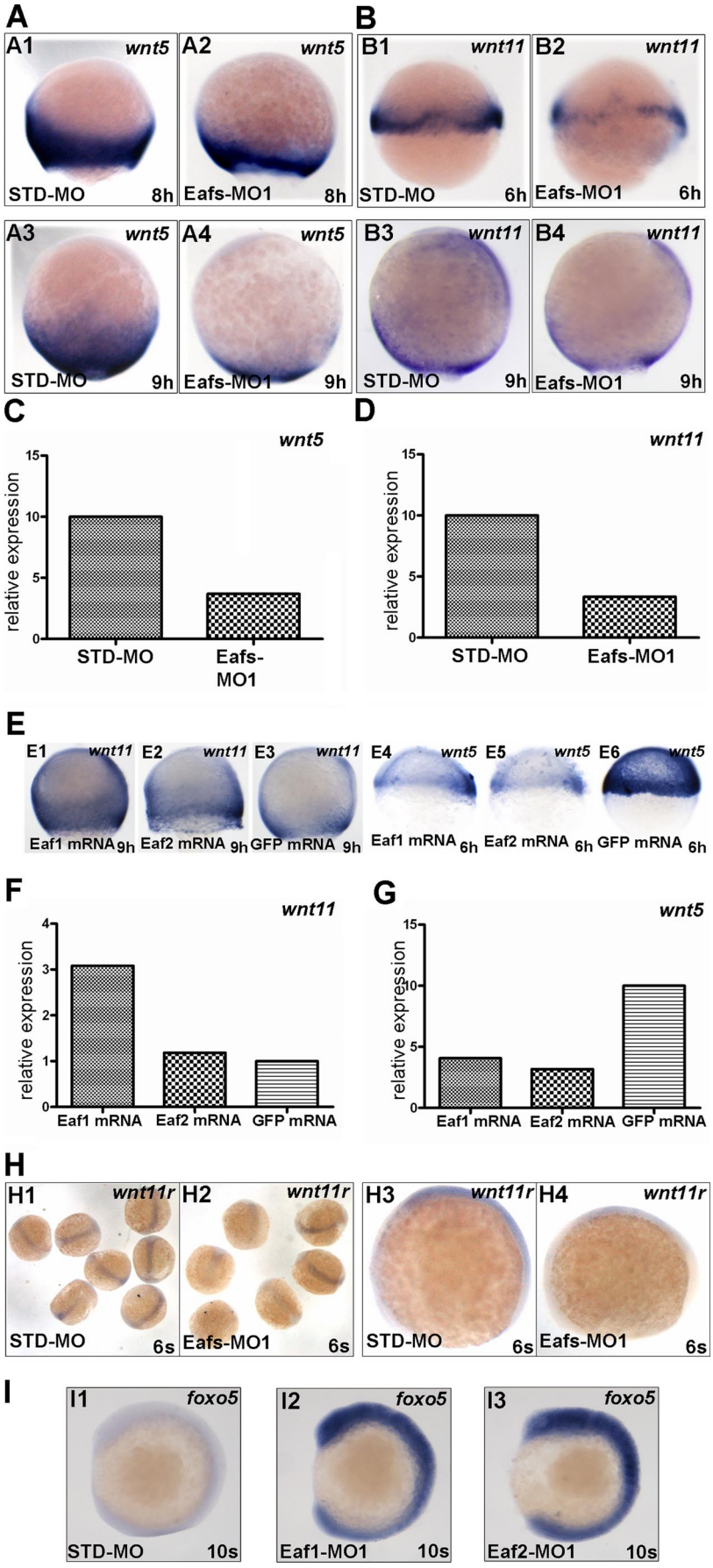

C4)) compared with the controls (Fig. 5*C* (*C1* and *C3*)). These results indicated that the specification of mesoderm occurred in *eafs* morphants, implying that the cell fate specification at the early gastrula was indeed not affected by *eafs* knockdown.

Furthermore, we examined the expression of three endoderm specification markers, including *foxa3*, *bon*, and *sox17*. As shown in Fig. 5*D*, the expression of *foxa3* in *eafs* morphants (Fig. 5*C* (*C2* and *C4*)) as well as that of *bon* (Fig. 3*E* (*E2*)) exhibited obviously expanded expression compared with the controls (Fig. 5, *D* (*D1* and *D3*) and *E* (*E1*)). The expression of another endoderm-specific gene, *sox17*, was also enriched at the ventro-lateral region in *eafs* morphants (Fig. 5*F* (*F2*)) compared with the controls (Fig. 5*F* (*F1*)). These results indicated that the specification of endoderm also occurred in *eafs* morphants, further suggesting that cell fate specification at early gastrula was not affected by *eafs* knockdown. Taken together, the knockdown of *eafs* did not affect cell fate specification at the beginning of gastrulation.

eaf1 and eaf2/u19 Are Required for the Midline Migration of Heart Precursors and Pancreas Precursors—During embryogenesis, the mesendoderm and midline structure strongly expressed *eaf1* and *eaf2/u19* transcripts (Fig. 1, *C* (*C3–C6*) and *D* (*D3–D6*)). We also observed that decrease in expression of these genes led to severe defects in convergence and extension movement (Figs. 2–4). Together, these findings suggest a role for Eaf1 and Eaf2/U19 in both cardiac and pancreas development. To assess this possibility, we used whole mount *in situ* hybridization to analyze expression of several cardiac markers, including *cmlc*, *bmp4*, *lefty2*, *vmhc*, and *amhc*. Both the *eaf1* and *eaf2/u19* morphants had a broader and more dispersed expression of *cmlc* than the control morphants (Fig. 6*A* (*A1–A3*)). However, loss of Eaf1 and Eaf2/U19 in *eafs* morphants resulted in the formation of two separate sites of *cmlc* expression (Fig. 6*A* (*A4*)). Similarly, both *bmp4* expression (Fig. 6*B* (*B2*)) and *amhc* expression (Fig. 6*E* (*E2*)) also separated into two parts in *eafs* morphants. In addition, the expression of *lefty2* (Fig. 6*C* (*C2*)) and *vmhc* (Fig. 6*D* (*D2*)) was much broader in *eafs* morphants as compared with control morphants. This evidence indicates that Eaf1 and Eaf2/U19 play very important roles in regulating the migration of cardiac cells.

To further explore whether the myocardial migration defects were a consequence of altered specification of myocardial precursors, we analyzed the expression levels of *gata5*, an early marker of myocardial specification. As shown in Fig. 6*F*, none of the embryos injected with Eaf1-MO1 (Fig. 6*F* (*F2*)), Eaf2-MO1 (Fig. 6*F* (*F3*)), or Eafs-MO1 (Fig. 6*F* (*F4*)) displayed significant changes in *gata5* expression levels, although heart primordia cells failed to converge at the midline under these experimental conditions. These results indicated that specification of the myocardial cell fate proceeded normally after ablation of Eaf1and Eaf2/U19 in embryos.

The migration of myocardial precursors toward the midline had been proposed to depend on endoderm specification (18)

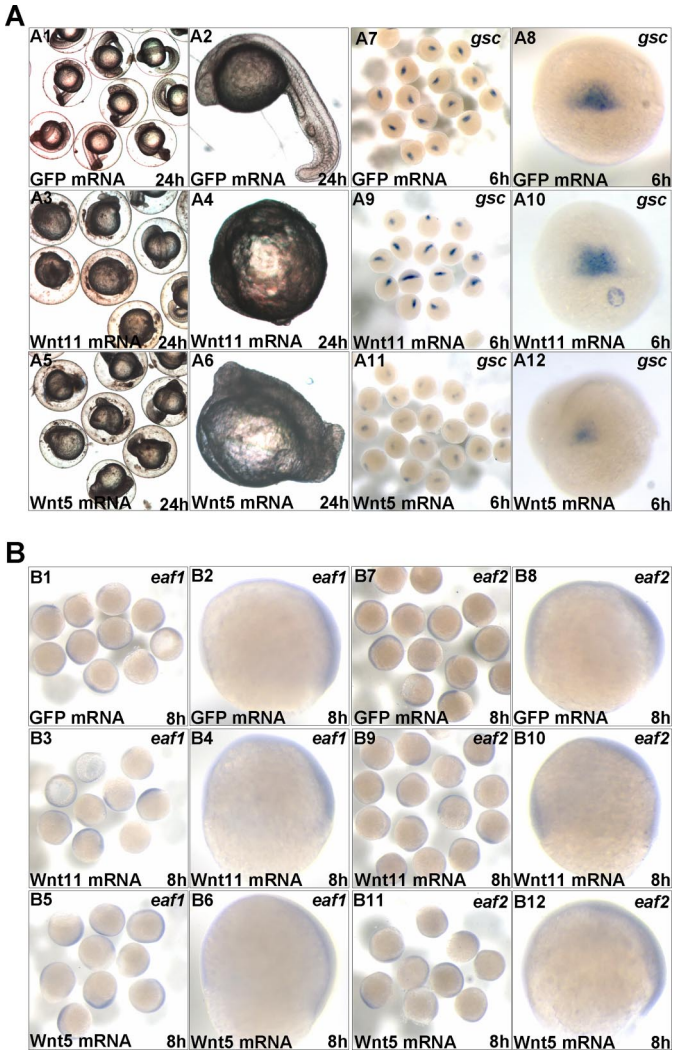

FIGURE 8. **The expression of *eaf1* and *eaf2/u19* was not affected by overexpression of *wnt5* and *wnt11*.** *A*, the functional evaluation of synthesized *wnt11* and *wnt5* mRNA. Embryos overexpressing *wnt11* were evaluated by morphology (*A3* and *A4*) and whole mount *in situ* hybridization (*gsc* staining) (*A9* and *A10*). Embryos overexpressing *wnt5* were evaluated by morphology (*A5* and *A6*) and whole mount *in situ* hybridization (*gsc* staining) (*A11* and *A12*). *B*, examination of *eaf1* and *eaf2/u19* expression in *wnt11*- and *wnt5*-overexpressed embryos by whole mount *in situ* hybridization. The expression pattern and level of *eaf1* and *eaf2/u19* (*B3*, *B4*, *B9*, and *B10*) were not changed in *wnt11*-overexpressing embryos compared with the control embryos injected with GFP mRNA (*B1*, *B2*, *B7*, and *B8*). The expression pattern and level of *eaf1* and *eaf2/u19* (*B5*, *B6*, *B11*, and *B12*) were not changed in *wnt5*-overexpressing embryos compared with the control embryos injected with GFP mRNA (*B1*, *B2*, *B7*, and *B8*).

FIGURE 7. **Eaf1 and *eaf2/u19* were required for maintaining *wnt5* and *wnt11* during gastrulation.** Shown are *wnt5* (*A*) and *wnt11* (*B*) expression in embryos injected with STD-MO or Eafs-MO1. In embryos with *eafs*-knockdown, the expression levels of both *wnt5* (*A2* and *A4*) and *wnt11* (*B2* and *B4*) were obviously lower than that of embryos injected with STD-MO (*A1*, *A3*, *B1*, and *B3*). Shown is *wnt5* (*C*) and *wnt11* (*D*) expression in embryos injected with STD-MO or Eafs-MO1, as determined by RT-PCR. *E*, overexpression of *eaf1* and *eaf2/u19* modulates *wnt5* and *wnt11* expression. Shown is a lateral view of *wnt11* (*E1–E3*) and *wnt5* (*E4–E6*) expression in embryos injected with *eaf1* mRNA (*E1* and *E4*), *eaf2/u19* mRNA (*E2* and *E5*), or GFP mRNA (control) (*E3* and *E6*), respectively. Shown are *wnt11* (*F*) and *wnt5* (*wnt5b*) (*G*) expression in embryos injected with *eaf1* mRNA, *eaf2/u19* mRNA, and GFP mRNA, as determined by RT-PCR. *H*, *wnt11r* expression in embryos injected with STD-MO (*H1* and *H3*) or Eafs-MO1 (*H2* and *H4*). *I*, *foxo5* expression in embryos injected with STD-MO (*I1*), Eaf1-MO1 (*I2*), or Eaf2-MO1 (*I3*).

or on midline convergence of the anterior endoderm (31); thus, we next investigated the effect of Eaf1 and Eaf2/U19 down-regulation on the expression of endoderm markers. Given that *gata5*, one of the earliest markers of endoderm fate determination (32) as well as a myocardial precursor marker, did not change in the *eafs* morphants (Fig. 6*F*), we evaluated markers of later stages in endoderm specification and pancreatic differentiation, *insulin* and *pdx-1*. Although the expression levels of *insulin* and *pdx-1* were similar between *eafs* morphants and control morphants, the pattern of expression varied (Fig. 6, *G*

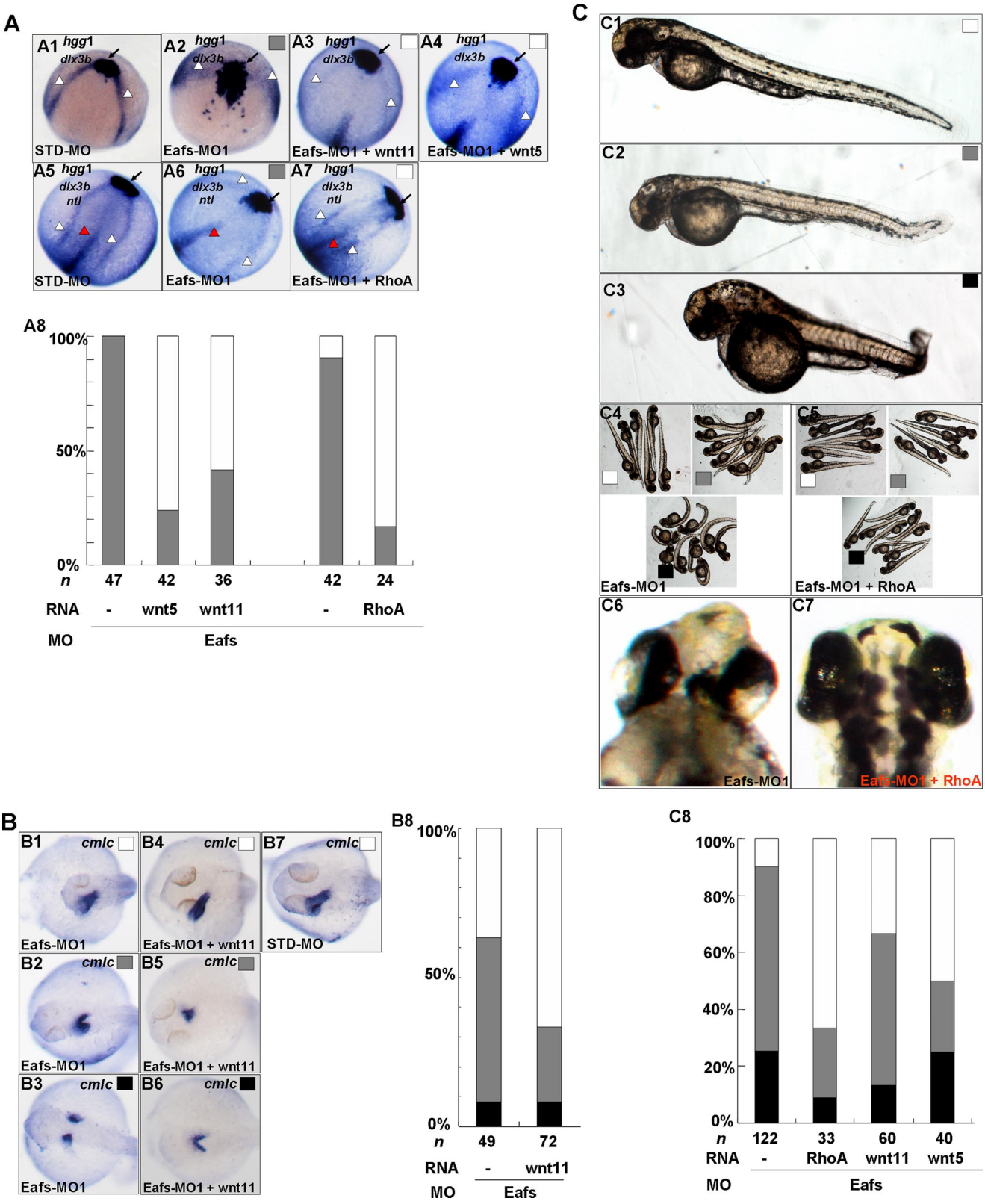

and *H*). Eaf1 and Eaf2/U19 knockdown resulted in the failure of fusion of the bilateral pancreas primordia, giving rise to a bifid pancreas (Fig. 6, *G* (*G2*) and *H* (*H2*)). Therefore, *eaf1* and *eaf2/u19* regulated midline convergence of organ primordia, including the heart and pancreas.

eaf1 and eaf2/u19 Regulate Expression of Noncanonical Wnt Ligands—Studies have shown that the noncanonical Wnt ligands, *wnt11* and *wnt5*, were functionally essential for the regulation of convergence and extension movement (20, 21, 33), and we have shown that *eafs* morphants phenocopied *wnt11* mutants and morphants, prompting us to investigate if *eaf1* and *eaf2/u19* affected convergence and extension movements through noncanonical Wnt signaling. Through *in situ* hybridization, we found that *wnt5 (wnt5b*) and *wnt11* transcripts were markedly reduced in Eafs-MO1-injected embryos as compared with STD-MO-injected embryos (Fig. 7, *A* and *B*). In addition, semiquantitative RT-PCR showed a remarkable decline in expression of both *wnt5* (Fig. 7*C*) and *wnt11* (Fig. 7*D*). We next investigated the expression level of *wnt5* and *wnt11* in embryos injected with *eaf1* and *eaf2/u19* mRNA. As compared with overexpression of ectopic GFP, overexpression of either *eaf1* or *eaf2/u19* mRNA led to a dramatic increase in *wnt11* mRNA in embryos, as determined by *in situ* hybridization and semiquantitative RT-PCR (Fig. 7, *E* (*E1* and *E2*) and *F*). Surprisingly, as with Eafs knockdown, overexpression *eaf1* or *eaf2/u19* down-regulated *wnt5* levels (Fig. 7, *E* (*E4* and *E5*) and *G*). These data suggest that *eaf1* and *eaf2/u19* act upstream of *wnt11* to regulate its expression, but the regulation of *wnt5* occurs through a different mechanism.

We have shown that *eaf1* and *eaf2/u19* contribute to midline convergence of organ precursors, a process regulated by the noncanonical Wnt ligands *wnt4a*, *wnt11*, and *wnt11r* (31). To establish if *eaf1* and *eaf2/u19* regulate expression of *wnt4a* and *wnt11r*, we measured expression in Eaf1 and Eaf2/U19 knockdown embryos. Eafs-MO1 injection produced a decrease in *wnt11r* levels (Fig. 7*H*) but an unexpected increase in *wnt4a*(*wnt4*) levels,[4] again underscoring the complexity of the signaling pathways.

It has been reported that *eaf1* and *eaf2/u19* could serve as regulators of transcriptional elongation by *in vitro* assays (7). This fact raised a question of whether the down-regulation of noncanonical Wnt ligands *wnt11*, *wnt5*, and *wnt11r* in *eafs* morphants was due to the disruption of the function of *eafs* in regulating transcriptional elongation. If this is the case, then *eafs* regulating *wnts* appears to be nonspecific. Although we already observed that the expression of a noncanonical Wnt ligand *wnt4a* was increased in *eafs* morphants, contrary to that of *wnt11*, *wnt5*, and *wnt11r*,[4] we still wanted to further clarify this issue. Through microarray analysis, we identified not only down-regulated genes but also up-regulated genes in *eafs* morphants.[5] From up-regulation genes, we chose *foxo5*, one of the highest up-regulated genes, for further verification by *in situ* hybridization. As shown in Fig. 7*I*, either Eaf1 or Eaf2/U19 knockdown could up-regulate *foxo5* expression (Fig. 7*I* (*I2* and *I3*)), similar to that of *wnt4a*,[4] which was also consistent with the data obtained from microarray analysis (data not shown). Thus, *eaf1* and *eaf2/u19* could also inhibit gene expression. Taken together, these observations ruled out the possibility that *eafs* regulating noncanonical Wnt ligands, *wnt11*, *wnt5*, and *wnt11r*, was nonspecific as a result of disrupting the activity of *eafs* for regulating transcriptional elongation in *eafs* morphants. Taking into consideration that the knockdown of *eafs* did not affect cell fate specification at early gastrula, we think that *eaf1* and *eaf2/u19* probably regulate noncanonical Wnt ligands specifically.

Expression of eaf1 and eaf2/u19 Is Not Affected by Overexpression of wnt11 and wnt5—To completely understand the relationship between noncanonical Wnt ligands (*wnt11* and *wnt5*) and the Eaf gene family, we set out to determine whether overexpression of *wnt11* or *wnt5* would have an impact on *eaf1* or *eaf2/u19* expression. First, we performed functional evaluation for synthesized zebrafish *wnt11* and *wnt5* mRNA. As showed in Fig. 8*A*, the embryos injected with either *wnt11* (Fig. 8*A* (*A3* and *A4*)) or *wnt5* mRNA (Fig. 8*A* (*A5* and *A6*)) exhibited malformed phenotypes as reported previously (34). In addition, compared with the control embryos injected with GFP mRNA (Fig. 8*A* (*A7* and *A8*)), the expression of organizer marker *gsc* reduced dramatically in embryos injected with *wnt5* mRNA (Fig. 8*A* (*A11* and *A12*)) but not in embryos injected with *wnt11* mRNA (Fig. 8*A* (*A9* and *A10*)), which was also consistent with the results reported previously (34, 35). These observations indicated that the synthesized *wnt11* and *wnt5* mRNA had

[4] X. Wan and W. Xiao, unpublished data.

[5] J.-X. Liu and W. Xiao, unpublished data.

FIGURE 9. ***wnt5*, *wnt11*, and *rhoA* partially rescued the defects of *eafs* morphants.** *A*, *wnt5*, *wnt11*, and *rhoA* partially rescued the convergence and extension movement defects of *eafs* morphants. Embryos were injected with STD-MO (*A1* and *A5*) or with Eafs-MO1 (*A2* and *A6*). *A3*, embryos were co-injected with Eafs-MO1 and *wnt11* mRNA (100 pg). *A4*, embryos were co-injected with Eafs-MO1 and *wnt5* mRNA (100 pg). *A7*, embryos were co-injected with Eafs-MO1 and *rhoA* mRNA (10 pg). *A1–A4*, 9 hpf, dorsal view, anterior to the *top right*; embryos were stained for *hgg1* and *dlx3b*. *A5–A7*, 12 hpf, dorsal view, anterior to the *top right*; the expression of *hgg1*, *dlx3b*, and *ntl* was stained. *Black arrow*, prechordal plate (stained by *hgg* probe); *white arrowhead*, edges of the neural plate (stained by *dlx3b*); *red arrowhead*, the axial chorda (stained by *ntl*). *A8*, the percentage of *eafs* morphants exhibiting convergence and extension movement defects was scored by the three markers: *hgg1*, *dlx3b*, and *ntl*. *Gray box*, defects; *white box*, wild-type or wild-type likely staining. *B*, *wnt11* partially rescued the defects of myocardial cell migration induced by Eafs-MO1 injection. *B1–B3*, 30 hpf embryos, injected with Eafs-MO1, stained by a *cmlc* probe, dorsal view, anterior to the *left*. *B4–B6*, 30 hpf embryos, co-injected with Eafs-MO1 and *wnt11* mRNA, stained by a *cmlc* probe, dorsal view, anterior to the *left*. *B7*, 30 hpf embryos, injected with STD-MO, stained by *cmlc* probe, dorsal view, anterior to the *left*. *B8*, the percentage of defects of myocardial cell migration in embryos injected with Eafs-MO1 alone or co-injected with Eafs-MO1 and *wnt11* mRNA based on the whole mount *in situ* hybridization assays. *White box*, wild-type or wild-type likely phenotypes; *gray box*, moderate defects; *black box*, severe defects. *C*, *rhoA*, *wnt5*, and *wnt11* rescued the general defects induced by Eafs-MO1 injection. *C1*, *C2*, and *C3*, 3 days postfertilization, the embryos were morphologically scored for defects into three categories: 1) wild-type, no discernable defect (*white box*); 2) moderate defect (*gray box*), characterized by slightly reduced head and anterior-posterior axis and slightly reduced distance between two eyes; and 3) severe defect (*black box*), characterized by dramatically reduced head and anterior-posterior axis and dramatically reduced distance between two eyes. *C4* and *C6*, embryos injected with Eafs-MO1. *C5* and *C7*, embryos co-injected with Eafs-MO1 and *rhoA* mRNA. *C8*, the embryos were scored morphologically; the percentages of WT (*white bar*), moderate (*gray bar*), and severe (*black bar*) are indicated. All of the injections, including MO alone or MO combined with mRNA, were performed using the same batch of embryos produced by a select number of zebrafish to eliminate the error caused by embryo variation.

intact function. Subsequently, we checked the expression of *eaf1* or *eaf2/u19* in embryos injected with either *wnt11* mRNA or *wnt5* mRNA. As showed in Fig. 8*B*, compared with the control embryos injected with GFP mRNA (Fig. 8*B* (*B1*, *B2*, *B7*, and *B8*)), both expression pattern and expression level of *eaf1* (Fig. 8*B* (*B3–B6*)) and *eaf2/u19* (Fig. 8*B* (*B9–B12*)) were not changed in *wnt11* and *wnt5* overexpression embryos. These results further suggested that *eaf1* and *eaf2/u19* function upstream of *wnt11* and *wnt5*.

eaf1 and eaf2/u19 Mediate Convergence and Extension Movements and Convergence of Organ Primordial through Wnt Signaling—To gain a better understanding of how *eaf1* and *eaf2/u19* may regulate convergence and extension movements during gastrulation, we performed rescue experiments using expression of *wnt11* and *wnt5* as well as wild-type *rhoA*, a down-stream gene of both *wnt5* and *wnt11*. We co-injected zebrafish embryos with Eafs-MO1 and *wnt5* mRNA, *wnt11* m*RNA*, or *rhoA* mRNA. We then scored embryos for expression of the convergence and extension movement markers *hgg1*, *dlx3b*, and *ntl* using *in situ* hybridization (Fig. 9*A*) as well as for general morphological characteristics (Fig. 9*C*). In *eafs* morphants, we found that *wnt11* mRNA not only suppressed the reduction in the anterior-posterior extension of the prechordal plate (Fig. 9*A* (*A3*), indicated by an *arrow*) but also suppressed cyclopia and body shortening (Fig. 9*C*). Furthermore, *wnt5* mRNA (Fig. 9, *A* (*A4*) and *C*) also rescued these defects effectively. Interestingly, *rhoA* rescued the defects even more effectively than *wnt11* and *wnt5*. In comparison with embryos injected with Eafs-MO1 alone (Fig. 9*A* (*A7*)), *rhoA*-rescued embryos exhibited a U-shaped prechordal plate with a normal anterior extension (Fig. 9*A* (*A7*), indicated by *arrows*). At the same time, both the edges of the neural crest (Fig. 9*A* (*A7*), indicated by *white triangles*) and notochord (Fig. 9*A* (*A7*), indicated by *red triangles*) narrowed in the embryos co-injected with *rhoA* mRNA (Fig. 9*A* (*A6*)). The cyclopia and shortened body defects seen in the *eafs* morphants were also significantly suppressed by co-injection of *rhoA* mRNA (Fig. 9*C* (*C5*, *C7*, and *C8*)). These results suggested that the ability of *eaf1* and *eaf2/u19* to govern convergence and extension movements during zebrafish gastrulation required the convergence of *wnt5* and *wnt11* on *rhoA*.

We also tested whether *eaf1* and *eaf2/u19* rely on noncanonical Wnt signaling to regulate convergence of organ primordia by co-injecting embryos with Eafs-MO1 and *wnt11* mRNA and then evaluating expression of the cardiac marker *cmlc*. In the 8.1% of *eafs* morphants exhibiting severe defects in myocardial cell migration, *cmlc* expression occurred in two separate locations (Fig. 9*B* (*B3* and *B8*)). *eafs* morphants with moderate defects, 55.1% in all, had a more dispersed *cmlc* expression (Fig. 9*B* (*B2* and *B8*)). Co-injection with *wnt11* mRNA widened the distance between the eyes in morphants with no discernable defects or moderate defects (Fig. 9*B* (*B4* and *B5*)). In the case of *eafs* morphants without discernable defects, co-injection with *wnt11* mRNA resulted in *cmlc* staining identical to that in the control morphants (Fig. 9*B* (*B4* and *B7*)). Introduction of ectopic *Wnt11* mRNA decreased the frequency of *eafs* morphants with moderate defects (22.2%; Fig. 9*B* (*B8*)), and in those morphants, the expression of *cmlc* was more concentrated (Fig. 9*B* (*B5*)). Last, in embryos co-injected with Eafs-MO1 and *wnt11* mRNA that exhibited severe defects, *cmlc* expression was only mildly bifida (Fig. 9*B* (*B6*)). These results suggested that *wnt11* mRNA could rescue the midline convergence defects of organ primordia induced by Eafs-MO1.

DISCUSSION

Previous studies have established that EAF2/U19 contributes to tumor suppression (9, 10). Other studies suggest that EAF1 and EAF2/U19, like other tumor suppressors, may play a role in vertebrate development (14, 15). However, their exact function in embryogenesis remains unclear. To better understand the cellular function of EAF1 and EAF2/U19 and subsequently how these proteins suppress tumors will require a more extensive investigation of their roles in embryogenesis. Here, we are the first to present data showing that *eaf1* and *eaf2/u19* mediate effective convergence and extension movements through the maintenance of *wnt11* and *wnt5* expression during zebrafish gastrulation.

Eaf family members demonstrated a high degree of conservation across species and with each other, so not surprisingly, the expression of *eaf1* and *eaf2/u19* observed in the zebrafish mirrored the pattern seen in the mouse (14). However, intercrosses of *EAF2/U19* heterozygous knock-out mice yielded *Eaf2/U19*-null offspring at Mendelian ratios at birth, suggesting that early mouse development did not require *EAF2/U19* (10). *Eaf2/U19* knockdown in zebrafish embryos alone caused defects in convergence and extension movements in our study. This phenotypic difference between mouse and zebrafish might result from either the redundant function of EAF1 and EAF2/U19 in mouse embryogenesis or from slightly different functions of EAF2/U19 in mammalians and lower vertebrate fish. Indeed, functional differences between mammalian and fish genes are not uncommon (36). In addition, *Eaf2/U19* knockdown in *Xenopus laevis* caused defects in eye development, which was a pure eye phenotype unrelated to the defect of convergence and extension movement (15). However, *eaf2/u19* knockdown in zebrafish caused shorter eye distance or eye fusion (partial cyclopia) resulting from the defect in convergence and extension movements (Fig. 8*C*). Together, *eaf1* and *eaf2/u19* might play different roles in eye development during embryogenesis. Further demonstrating the different mechanism of *eaf1* and *eaf2/u19* playing their roles in eye formation among species probably will give us a more complete picture about the function of *eaf1* and *eaf2/u19* in embryogenesis.

eaf1 and *eaf2/u19* appeared to play partially redundant roles in the regulation of convergence and extension movements. Knockdown of both *eaf1* and *eaf2/u19* resulted in abnormal cell behavior in both the head and trunk mesendoderm (Fig. 2). The phenotypes observed in *eafs* morphants included disorganized head structure, reduced body axis, and shorter tail and were similar to those seen in embryos with a disruption of convergence and extension movements (20, 21, 33, 37–39). On the basis of phenotype, the marker gene expression patterns, and cell tracing experiments, we concluded that *eaf1* and *eaf2/u19* served as novel regulators of convergence and extension movements (Figs. 2–4). In reciprocal rescue experiments, *eaf1* mRNA could rescue Eaf2-MO1 knockdowns, and *eaf2/u19*

mRNA could rescue Eaf1-MO knockdowns, suggesting redundant roles for Eaf1 and Eaf2/U19 in the regulation of convergence and extension movements. However, knockdown of either *eaf1* or *eaf2/u19* produced similar defects that increased in severity with the combined knockdown of both Eaf1 and Eaf2/U19 (Figs. 2–4), indicating that these proteins do not have completely redundant functions.

In this study, we found that *eaf1* and *eaf2/u19* might contribute to the regulation of convergence and extension movements through noncanonical Wnt signaling. Eaf1 and Eaf2/U19 knockdown dramatically down-regulated *wnt11* expression, whereas introduction of ectopic *eaf1* and *eaf2/u19* mRNA increased *wnt11* expression (Fig. 7). Moreover, *wnt11* mRNA rescued convergence and extension movement defects caused by Eaf1 and Eaf2/U19 knockdown with high frequency (Fig. 9*A*). However, overexpression of *wnt11* by mRNA injection did not affect the expression of *eaf1* and *eaf2/u19* (Fig. 8). These findings imply that *eaf1* and *eaf2/u19* act upstream of *wnt11* to control its expression and to govern convergence and extension movements. Furthermore, Eaf1 and Eaf2/U19 knockdown down-regulated *wnt5* expression (Fig. 7, *A* and *C*), and *wnt5* mRNA, in turn, also rescued defects in convergence and extension movements caused by the loss of *eaf1* and *eaf2/u19* (Fig. 9*A* (*A4*)). However, overexpression of *eaf1* and *eaf2/u19* also down-regulated *wnt5* expression, with expression levels comparable with those seen in the *eafs* morphants (Fig. 7, *E* and *G*). This suggests that the maintenance of *wnt5* might require a specific level or ratio of *eaf1* and *eaf2/u19*. Similar to that of *wnt11*, *wnt5* overexpression did not affect the expression of *eaf1* and *eaf2/u19*, suggesting that *eaf1* and *eaf2/u19* also act upstream of *wnt5*. As a downstream activator of noncanonical Wnt ligands, RhoA rescued convergence and extension movement defect more effectively than Wnt5 and Wnt11 (Fig. 8), indicating a convergence of *wnt5* and *wnt11* on *rhoA* during the regulation of convergence and extension movements. Of note, the expression patterns of *eaf1* and *eaf2/u19* were similar to that of *rhoA* during zebrafish and *Xenopus* embryogenesis (22, 40).

Notably, *eaf1* and *eaf2/u19* have activity in stimulating ELL transcriptional elongation (7). Thus, if knockdown of *eaf1* and *eaf2/u19* only caused inhibition of gene expression, *eafs* regulating the expression of Wnts (*wnt11*, *wnt5*, and *wnt11r*) presented in this study might be nonspecific as a result of disrupting the general function of *eafs* as regulators of transcriptional elongation. However, in addition to *wnt4a*,[4] *foxo5* (Fig. 9*A*) as well as other genes[5] were up-regulated by *eafs* knockdown, unrelated to their function as regulators of transcriptional elongation. Therefore, *eafs* knockdown inhibiting the expression of *Wnts* appears to be specific. Taking into consideration that the knockdown of *eafs* did not affect cell fate specification at the beginning of gastrulation, it suggests that *eafs* might directly regulate noncanonical Wnt ligands (especially for *wnt11*). However, this conclusion needs to be further verified by more direct ways, such as promoter chromatin immunoprecipitation assays, etc.

Knockdown of Eaf1 and Eaf2/U19 protein levels also resulted in the failure of fusion of the heart and pancreas primordia (Fig. 6), but neither endoderm fate determination genes nor myocardial precursor marker genes displayed significant changes in their expression levels (Fig. 6, *F–H*). These observations imply that *eaf1* and *eaf2/u19* act as novel regulators of midline convergence of both endoderm- and mesoderm-derived organ primordia without affecting the specification of progenitors.

Although a primary role of non-canonical Wnt signaling was to govern convergence and extension movements, studies had also shown that the three Wnt noncanonical ligands, *wnt4a*, *wnt11*, and *wnt11r*, redundantly regulated midline convergence of organ primordia, in zebrafish embryos (31, 41). In this study, we showed that the midline migration of heart precursors and pancreas precursors required expression of *eaf1* and *eaf2/u19* (Fig. 6). We also showed that *eaf1* and *eaf2/u19* mediated midline convergence through noncanonical Wnt signaling, specifically by regulating expression of *wnt11* and *wnt11r* (Figs. 7 and 9). Unexpectedly, however, knockdown of *eaf1* and *eaf2/u19* up-regulated *wnt4a* expression.[4] This observation suggested that, unlike *wnt11* and *wntllr*, *wnt4a* was not a downstream factor of *eaf1* and *eaf2/u19* in the signaling pathway that regulated midline convergence of organ precursors.

In conclusion, our data are the first to demonstrate that *eaf1* and *eaf2/u19* have essential roles in regulating embryonic cell behavior and migration. Although the complete pathway has yet to be defined, our study shows that *eaf1* and *eaf2/u19* function in this pathway by specifically modulating expression of *wnt11* and *wnt5*, which in turn converge on *rhoA* for the positive regulation of convergence and extension movements.

Acknowledgments—We thank Drs. Zhan Yin, Yonghua Sun, and T. Whitfield for the generous gifts of various reagents. We also thank Moira Hitchens for editing.

REFERENCES

1. Thirman, M. J., Levitan, D. A., Kobayashi, H., Simon, M. C., and Rowley, J. D. (1994) *Proc. Natl. Acad. Sci. U. S. A.* **91,** 12110–12114
2. Simone, F., Polak, P. E., Kaberlein, J. J., Luo, R. T., Levitan, D. A., and Thirman, M. J. (2001) *Blood* **98,** 201–209
3. Wang, Z., Tufts, R., Haleem, R., and Cai, X. (1997) *Proc. Natl. Acad. Sci. U. S. A.* **94,** 12999–13004
4. Simone, F., Luo, R. T., Polak, P. E., Kaberlein, J. J., and Thirman, M. J. (2003) *Blood* **101,** 2355–2362
5. Shilatifard, A., Lane, W. S., Jackson, K. W., Conaway, R. C., and Conaway, J. W. (1996) *Science* **271,** 1873–1876
6. Mitani, K., Yamagata, T., Iida, C., Oda, H., Maki, K., Ichikawa, M., Asai, T., Honda, H., Kurokawa, M., and Hirai, H. (2000) *Biochem. Biophys. Res. Commun.* **279,** 563–567
7. Kong, S. E., Banks, C. A., Shilatifard, A., Conaway, J. W., and Conaway, R. C. (2005) *Proc. Natl. Acad. Sci. U. S. A.* **102,** 10094–10098
8. Luo, R. T., Lavau, C., Du, C., Simone, F., Polak, P. E., Kawamata, S., and Thirman, M. J. (2001) *Mol. Cell. Biol.* **21,** 5678–5687
9. Xiao, W., Zhang, Q., Jiang, F., Pins, M., Kozlowski, J. M., and Wang, Z. (2003) *Cancer Res.* **63,** 4698–4704
10. Xiao, W., Zhang, Q., Habermacher, G., Yang, X., Zhang, A. Y., Cai, X., Hahn, J., Liu, J., Pins, M., Doglio, L., Dhir, R., Gingrich, J., and Wang, Z. (2008) *Oncogene* **27,** 1536–1544
11. Xiao, W., Ai, J., Habermacher, G., Volpert, O., Yang, X., Zhang, A. Y., Hahn, J., Cai, X., and Wang, Z. (2009) *Cancer Res.* **69,** 2599–2606
12. Lee, H., and Kimelman, D. (2002) *Dev. Cell* **2,** 607–616
13. Langheinrich, U., Hennen, E., Stott, G., and Vacun, G. (2002) *Curr. Biol.* **12,** 2023–2028
14. Li, M., Wu, X., Zhuang, F., Jiang, S., Jiang, M., and Liu, Y. H. (2003) *Dev.*

Dyn. **228,** 273–280
15. Maurus, D., Héligon, C., Bürger-Schwärzler, A., Brändli, A. W., and Kühl, M. (2005) *EMBO J.* **24,** 1181–1191
16. Myers, D. C., Sepich, D. S., and Solnica-Krezel, L. (2002) *Trends Genet.* **18,** 447–455
17. Keller, R., Shih, J., and Domingo, C. (1992) *Dev. Suppl.* 81–91
18. Stainier, D. Y. (2001) *Nat. Rev.* **2,** 39–48
19. Ober, E. A., Olofsson, B., Mäkinen, T., Jin, S. W., Shoji, W., Koh, G. Y., Alitalo, K., and Stainier, D. Y. (2004) *EMBO Rep.* **5,** 78–84
20. Heisenberg, C. P., Tada, M., Rauch, G. J., Saúde, L., Concha, M. L., Geisler, R., Stemple, D. L., Smith, J. C., and Wilson, S. W. (2000) *Nature* **405,** 76–81
21. Kilian, B., Mansukoski, H., Barbosa, F. C., Ulrich, F., Tada, M., and Heisenberg, C. P. (2003) *Mech. Dev.* **120,** 467–476
22. Zhu, S., Liu, L., Korzh, V., Gong, Z., and Low, B. C. (2006) *Cell. Signal.* **18,** 359–372
23. Westerfield, M., Doerry, E., and Douglas, S. (1999) *Trends Genet.* **15,** 248–249
24. Kimmel, C. B., Ballard, W. W., Kimmel, S. R., Ullmann, B., and Schilling, T. F. (1995) *Dev. Dyn.* **203,** 253–310
25. Hammond, K. L., Loynes, H. E., Folarin, A. A., Smith, J., and Whitfield, T. T. (2003) *Development* **130,** 1403–1417
26. Yang, Z., Liu, N., and Lin, S. (2001) *Dev. Biol.* **231,** 138–148
27. Ando, R., Hama, H., Yamamoto-Hino, M., Mizuno, H., and Miyawaki, A. (2002) *Proc. Natl. Acad. Sci. U. S. A.* **99,** 12651–12656
28. Jopling, C., and den Hertog, J. (2005) *EMBO Rep.* **6,** 426–431
29. Jopling, C., van Geemen, D., and den Hertog, J. (2007) *PLoS Genet.* **3,** e225
30. Jopling, C., and Hertog, J. (2007) *Mech. Dev.* **124,** 129–136
31. Matsui, T., Raya, A., Kawakami, Y., Callol-Massot, C., Capdevila, J., Rodríguez-Esteban, C., and Izpisúa Belmonte, J. C. (2005) *Genes Dev.* **19,** 164–175
32. Reiter, J. F., Kikuchi, Y., and Stainier, D. Y. (2001) *Development* **128,** 125–135
33. Wallingford, J. B., Fraser, S. E., and Harland, R. M. (2002) *Dev. Cell* **2,** 695–706
34. Westfall, T. A., Brimeyer, R., Twedt, J., Gladon, J., Olberding, A., Furutani-Seiki, M., and Slusarski, D. C. (2003) *J. Cell Biol.* **162,** 889–898
35. Tao, Q., Yokota, C., Puck, H., Kofron, M., Birsoy, B., Yan, D., Asashima, M., Wylie, C. C., Lin, X., and Heasman, J. (2005) *Cell* **120,** 857–871
36. Correa, R. G., Matsui, T., Tergaonkar, V., Rodriguez-Esteban, C., Izpisua-Belmonte, J. C., and Verma, I. M. (2005) *Curr. Biol.* **15,** 1291–1295
37. Yamashita, S., Miyagi, C., Carmany-Rampey, A., Shimizu, T., Fujii, R., Schier, A. F., and Hirano, T. (2002) *Dev. Cell* **2,** 363–375
38. Topczewski, J., Sepich, D. S., Myers, D. C., Walker, C., Amores, A., Lele, Z., Hammerschmidt, M., Postlethwait, J., and Solnica-Krezel, L. (2001) *Dev. Cell* **1,** 251–264
39. Jessen, J. R., Topczewski, J., Bingham, S., Sepich, D. S., Marlow, F., Chandrasekhar, A., and Solnica-Krezel, L. (2002) *Nat. Cell Biol.* **4,** 610–615
40. Wünnenberg-Stapleton, K., Blitz, I. L., Hashimoto, C., and Cho, K. W. (1999) *Development* **126,** 5339–5351
41. Miyasaka, K. Y., Kida, Y. S., Sato, T., Minami, M., and Ogura, T. (2007) *Proc. Natl. Acad. Sci. U. S. A* **104,** 11274–11279